IIETA International Information and Engineering Technology Association
Advancing the World of Information and Engineering

Traitement du Signal
Vol. 40, No. 2, April, 2023, pp. 667-674
Journal homepage: http://iieta.org/journals/ts

Content-Based Image Recovery System with the Aid of Median Binary Design Pattern

Abolfazl Mehbodniya[1*], Julian Webber[1], Appari Geetha Devi[2], Rajendra Prasad Somineni[3], Mangali Chinna Chinnaiah[4], Anju Asokan[5], Koka Shamshad Bhanu[6]

[1] Department of Electronics and Communication Engineering, Kuwait College of Science and Technology (KCST), Doha Area, 7th Ring Road, Kuwait City 4600, Kuwait
[2] Department of Electronics and Communication Engineering, PVP Siddhartha Institute of Technology, Vijayawada 520007, Andhra Pradesh, India
[3] Department of Electronics and Communication Engineering, VNR Vignana Jyothi Institute of Engineering and Technology, Telangana 500090, India
[4] Department of Electronics and Communication Engineering, B V Raju Institute of Technology, Narsapur, Medak, Telangana 500082, India
[5] Department of Computer and Communication Engineering, Sri Eshwar College of Engineering, Coimbatore 641202, India
[6] Department of Electronics and Communication Engineering, Dr. K. V. Subba Reddy Institute of Technology, Kurnool 518218, Andhra Pradesh, India

Corresponding Author Email: a.niya@kcst.edu.kw

https://doi.org/10.18280/ts.400225

Received: 22 October 2022
Accepted: 13 March 2023

Keywords:
content-based image recovery (CBIR), local binary pattern (LBP), median binary pattern (MBP), multichannel decode local binary pattern (mdLBP), average recovery rate (ARR), average precision rate (APR)

ABSTRACT

Content-based image retrieval is a technique for locating images in vast, unlabeled image collections (CBIR). However, users are not happy with the traditional methods of information retrieval. Additionally, the number of consumer-accessible pictures and online production and distribution channels are expanding. Consequently, permanent and widespread digital image processing occurs across numerous industries. As a result, acquiring quick access to these big image databases and extracting identical images from sizable groups of photographs from a specific image (Query) create significant problems that call for efficient solutions. Calculations related to similarity and feature representation are crucial to a CBIR system's effectiveness. Color, shape, texture, and gradient are some essential features that can be utilized to portray an image. Local Binary Pattern (LBP) is a modest and successful texture controller that marks the pixels of an image by controlling the part of every pixel and deciphering the outcome as a binary value. The Local Binary Pattern (LBP) approach is acquainted with grey-level images to characterize color images as the pattern's dimensionality is enhanced. The current study proposes the 'Median Binary Pattern', which incorporates the multichannel decoded Local Binary Pattern (mdLBP) utilized to portray color images. For consolidating LBPs from more than one channel to make the descriptor noise-robust, two structures, specifically adder and decoder-based structures, and a noise-robust binary pattern called the 'Median Binary Pattern'. Compared with existing approaches, the proposed method achieved Average Recovery precision (ARP) and Average Recovery rate (ARR) of 68.1 and 33.55, respectively, with Noise Robust Binary Patterns.

1. INTRODUCTION

Multimedia data, such as films and photographs, have significantly risen in our daily lives along with the growth and use of the Internet [1]. Today, a popular research area is the speedy and accurate retrieval of important information in mass multimedia. Content-based image retrieval (CBIR) is one of the most well-liked fundamental research fields. Although CBIR has seen a lot of research activity during the 1990s, the complexity of image data continues to present several complex problems [2]. These problems are associated with difficulties in several interdisciplinary study fields, including computer vision, image processing, image databases, machine learning, etc. [3, 4].

Unlike conventional keywords-based image retrieval, a typical CBIR retrieves images based on their visual content, such as color, form, and texture, etc. [5]. There are numerous CBIR methodologies, and practically all of them adhere to a standardized CBIR pipeline. The pipeline's first step is extracting features from the photo group [6-8]. Typically, only one instance of this step is required to produce a feature database. The database can be regenerated if there are new photographs in the collection [9]. Any data that can be calculated from an image's pixels and is pertinent to the image is referred to as a feature. A feature vector is created by organizing these features [10].

Figure 1. Sample images for CBIR

An input image is the first step in a CBIR pipeline inquiry. A feature vector is generated when features are extracted from this image [11]. Only feature vectors with a proximity to the input vector are returned after the input feature vector has been compared to every feature vector in the database. A method's success depends on how the distance is calculated [12]. Sample images of CBIR is shown in Figure 1.

Existing approaches cannot efficiently use the saliency zones of images, and human perception of images cannot be well stored [13, 14]. In addition, typical feature extraction techniques overlook the spatial structure of images, which is an essential quality for image retrieval [15-17]. Another popular feature is texture. Traditional approaches, including the Tamura texture feature, GLCM and Gabor filter texture feature, are used to define texture features. When compared to the suggested methodology, the method and its considerable computing complexity produce poor results [18, 19].

To solve these limitations, we propose a novel image retrieval method based on a multichannel decode local-binary pattern is recommended. To consolidate the LBPs from each channel of color images, this method utilizes adder and decoder-based techniques and functions admirably with color images. This paper proposes the median binary pattern (MBP), famous for its noise-resilient binary pattern, to make the framework noise-resilient.

Further content of this research work is systematized as Section-II examines interrelated work, Section-III talks about existing techniques, Section-IV discusses proposed strategies, Section-V examines test results and examinations, and Section-VI talks about the proposed strategy's conclusion and future extension.

2. RELATED WORK

For a long time, various techniques have been implemented for effective content-based image recovery.

To learn more effective convolutional models for Content-Based Image Retrieval, Tzelepi and Tefas [19] offer a model retraining strategy. A deep CNN method extracts the feature representations from the convolutional layer activations then they adapt and retrain the network to generate more effective compact image descriptors. When compared with existing approaches, the proposed method shows superior performance.

Saritha et al. [20] combine the features of the color histogram, edge, edge directions, edge histogram, and texture features, among others, to propose a multi-feature picture retrieval technique. The content-based image will be selected from a list of this model's planned image groups. After performing preprocessing procedures such as selection removal, the traits mentioned above are extracted and saved as small signature files. The suggested method outperforms the current one.

Deep convolutional neural network-based self-supervised image retrieval system AutoRet is introduced by Monowar et al. [21]. Pairwise constraints are used to train the system. As a result, it can operate under its supervision and be educated on partially labeled data. A DCNN that extracts embedding's from various image patches is part of the overall method. Additionally, the embeddings are combined to provide high-quality data that is employed in the picture retrieval process.

Yousuf et al. [22] present a sophisticated method for improving CBIR effectiveness based on the visual fusion of SIFT and LIOP descriptors. On scale changes and constant rotations, SIFT outperforms. However, LIOP outperforms SIFT when there is little contrast and variations in illumination inside a picture. Even with significant rotation and scale changes, SIFT performs better than LIOP, which struggles under these conditions. The suggested method resolves the abovementioned problems and noticeably boosts CBIR effectiveness because it is based on the visual word fusion of SIFT and LIOP descriptors.

By effectively fusing two different types of histograms retrieved from color and local directional pattern (LDP), Zhou et al. [23] present a novel method for retrieving color images. They begin by outlining the color histogram and LDP extraction procedure. Then, after presenting these two features, we create a successful fusion method that incorporates feature normalization and a new similarity measure. This novel methodology is valid after comparing current state-of-the-art methods on two benchmark datasets.

When consumers search for photos from a sizable image collection or the World Wide Web, image search engines become essential tools. Its primary method is content-based image retrieval (CBIR), which enables users to look up photos using automatically generated attributes like color, texture, or shape. The significant disconnect between low-level image characteristics and high-level image semantics is the main challenge of CBIR. To overcome this challenge, we present novel research.

3. PROPOSED METHOD

The noise in digital images is mainly developed in the course of image procurement or image sharing. Because of the image noise, one can't distinguish the data in images. There are countless reasons for noise in images, like ecological conditions at the time of image procurement or based on the nature of the detecting components. The primary cause for noise in the image is interfering with the channel applied for image sharing. Noise image can be demonstrated below,

$$A(x,y) + B(x,y) = C(x,y) \quad (1)$$

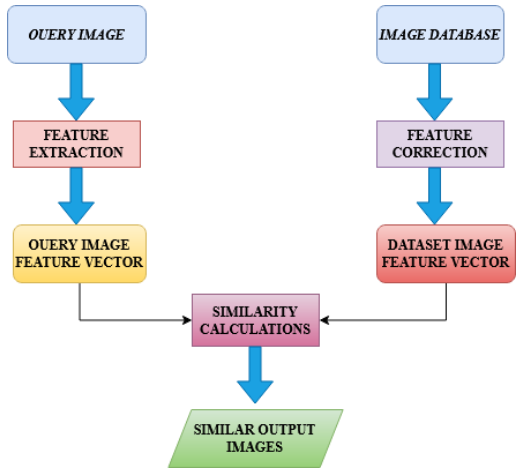

Figure 2. The layout of the content-based image recovery process

Here $A(x, y)$ addresses the first image pixel worth and $B(x, y)$ is the noise found in the image, and $C(x, y)$ is the subsequent noise image. Salt and pepper noise is used for the analyses in the present paper. The filtering method utilized in this paper is

Median Binary Pattern (MBP). Middle Binary Pattern (MBP) administrator maps the concentration space to the local binary pattern (LBP) by developing the pixels. MBP generated pattern is utilized to describe color images. For the effective utilization of the LBP data from different channels, two multichannel decoded LBP methods are suggested in this paper: multichannel adder-based LBP (maLBP) and multichannel decoder-based LBP (mdLBP). The proposed approach was tested using image recovery on the Corel 1k dataset. Five classes were considered: beaches, monuments, buses, dinosaurs, and elephants, each with 20 images. Figure 2 explains the proposed architecture.

3.1 Problem statement

Given that the color histogram is a statistical result and has the advantages of being straightforward, reliable, and effective, it is acknowledged as a suitable representation of features. However, the fundamental issue with color histogram indexing is that it ignores spatial information. A system that handles any image of a user's interest as a query image and compares the image with the data to obtain precise matches or photos in the same general category as the query images is to be built. The construction of a system that admits any image as a query image and retrieves images by analyzing or matching image data using specific properties of the image offers a solution to the problem statement. These characteristics are derived from the saliency maps-based method of salient feature extraction.

3.2 Salt and pepper noise

This kind of noise is known as gunshot noise, spike noise, or impulse noise [10, 11], which is generally affected by wrong retention areas, failure of pixel constituents in the camera sensors, or there may be mistakes in timing during digitization. To mitigate noise, filtering methods are utilized. The filtering method used in this paper is Median Binary Pattern (MBP).

3.3 Middle Binary Pattern (MBP)

Middle Binary Pattern (MBP) [17, 18] is the method utilized to control the noise present in the image. Middle Binary Pattern (MBP) administrator maps the concentration space to the local binary pattern (LBP) by developing the pixels in contrast to their median value in a (normally 3×3) neighborhood rather than continually utilizing the middle pixel as I LBP to give greater affectability to noise robustness. The median value of 120 is observed in the patch. The MBP at pixel (*x*, *y*) is characterized as,

$$\mathrm{MBP(i,j)} = \sum_{k=0}^{L-1} 2^K H(b_k - \tau) \qquad (2)$$

where, L is the patch size or pixel area (i.e., L=9 for 3X3 fix) and τ to is the middle of the patch.

The MBP is utilized to measure the supply of these patterns in the image and structures the surface descriptor in Figure 4.

As indicated by the meaning of the LBP, an $LBPt\ (x, y)$ for a specific pixel (x, y) in t[th] network is created by figuring out a binary number $LBPtn\ (x, y)$ assumed in the below formula,

$$LBPt\ (x,y) = \sum_{n=1}^{N} LBP_t^n\ (x,y) \times f^n, for\ all\ t[1,c]$$

where, f^n is $LBP_t^n\ (x,y) = \begin{cases} 1, & I_t^n(x,y) \geq I_t(x,y) \\ 0, & \text{Otherwise} \end{cases}$ a premium task demarcated by the succeeding formula $f^n = (2)^{(n-1)}$ for all $n \in [1, N]$. Figure 3 represents the block diagram of median binary pattern.

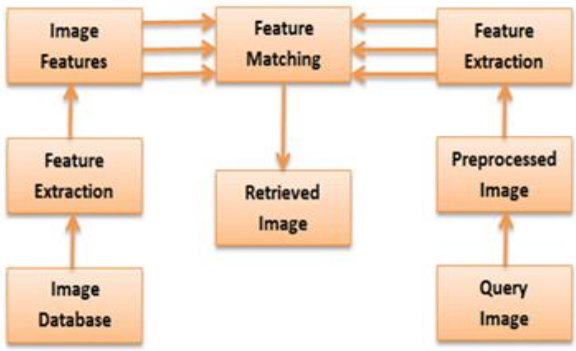

Figure 3. Block diagram of median binary pattern

Figure 4. MBP for a 3×3 patch (i.e., L=9) with a median τ=120 output binary pattern MBP=100011110_2 =286

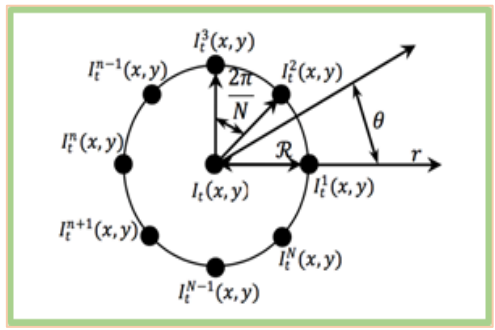

Figure 5. The local neighbors
Image Source: https://github.com/arorayash/mdLBP

The N binary values *LBPtn*(*x*, *y*) is set in a specific pixel of (*x*, *y*) relating to every neighbor *Itn*(*x*, *y*) of t[th] channel. Local neighbors of MBP were represented in Figure 5.

3.4 Multichannel Decoded Local Binary Pattern (mdLBP)

This pattern is utilized to describe color images. For the effective utilization of the LBP data from different channels, two multichannel decoded LBP [2, 15] methods are suggested in this paper: multichannel adder-based LBP (maLBP) and multichannel decoder-based LBP (mdLBP). A sum of (c+1) element and (2c) of resulted channels are created as of (c) number of input-based channels of (c≥2) utilizing a multichannel adder and decoder, respectively. Image 4 portrays the calculation interaction engaged with multichannel adder-based and decoder-based LBPs. Multichannel LBP adders and decoders are utilized to describe the color images, with *LBPtn*(*x*, *y*) for all $t \in -[1, c]$ as the c input-based

channels. Hence the results of multichannel adder-based and multichannel decoder-based local binary patterns are indicated by *maLBPt1n*(*x*, *y*) and *mdLBPt2n*(*x*, *y*), separately, $t1 \in [1, c+1]$and $t2 \in [1,2c]$. It ought to be noticed that the calculated numbers of *LBPtn*(*x*, *y*) may be binary values (for example, 0 or 1). Consequently, the binary numbers of *maLBPt1n*(*x*, *y*) & *mdLBPt2n*(*x*, *y*) have resulted from the multichannel adder map and multichannel decoder map decoded by *maMn*(*x*, *y*) & *mdMn*(*x*, *y*) relating to every pixel's neighbor *n*.(*x*, *y*). Numerically, *maMn*(*x*, *y*) & *mdMn*(*x*, *y*) are characterized as follows:

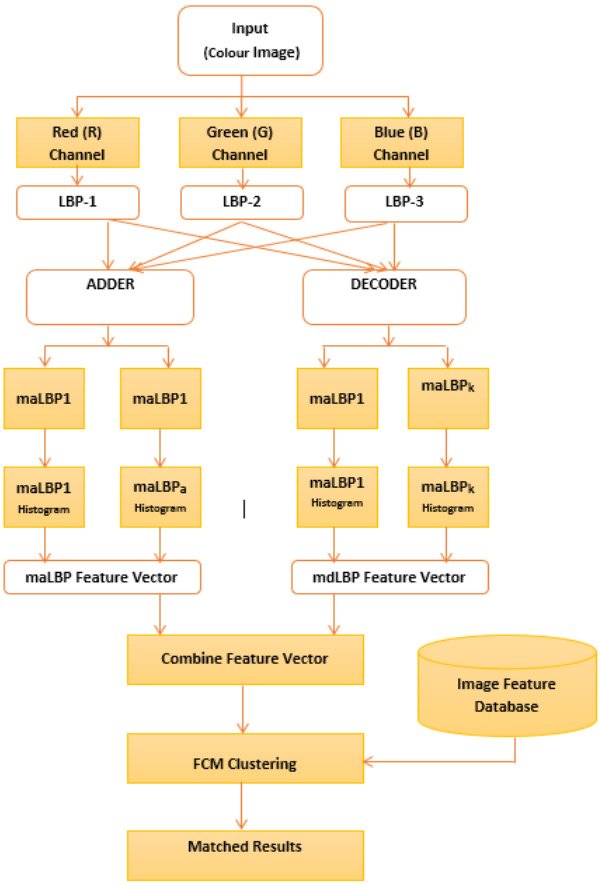

Figure 6. Flowchart of a mix of multichannel adder

Figure 6 shows the LBP highlight vector (for example, maLBP) and multichannel decoder-based LBP highlight vector (for example, mdLBP) of the picture's blue, red, and green channels. We denote $\mathrm{LBP}_t^n(x,y)$ of all $n \in -[1,N]$ in a same way for all the $t \in -[1,c+1]$ in adder pattern and $mdLBP_{t2^n}(x,y)$ for all $n \in -[1,N]$ and $t_2 \in [1,2^c]$ in decoder pattern correspondingly. The multi-channel adder-based LBP $maLBP_{t1^n}(x,y)$ for pixel (x, y) from multi-channel adder map $maM^n(x,y)$ and t_1 is defined as,

$$mdLBP_{t1}^n(x,y) = \begin{cases} 1, & maM^n(x,y) \geq (t_1 - 1) \\ 0, & \text{otherwise} \end{cases} for\ all\ t_2 \in [1, c+1] and\ for\ all\ n \in [1,N]. \quad (3)$$

Multi-channel decoder map mdMn (*x*, *y*) and t_2 may be calculated as,

$$mdLBP_{t2}^n(x,y) = \begin{cases} 1, & mdM^n(x,y) \geq (t_2 - 1) \\ 0, & \text{otherwise} \end{cases} \quad (4)$$

$$for\ all\ t_2 \in [1,2^c] and\ for\ all\ n \in [1,N]$$

The computation of $maLBP_{t1}(x,y)$ for all $t1 \in -[1,c+1]$ in the same way $maLBP_{t2}(x,y)$ for all $t_2 \in [1,2^c]$ from input $LBP_{t^n}(x,y)$ applying a sample as shown in Figure 7 for c=3 and N=8.

The multi-channel adder based LBPs ($maLBP_{t1}(x,y) for\ all\ t1 \in -[1,c+1]$) for the middle pixel (*x*, *y*) is calculated by applying $maLBP_{t1^n}(x,y)$ is defined as,

$$maLBP_{t1}(x,y) = \sum_{n=1}^{N} maLBP_{t1^n}(x,y) \times f^n \quad (5)$$

And multi-channel decoder based LBPs ($mdLBP_{t2}(x,y)\ for\ all\ t2 \in [1,2^c]$) is calculated for the middle pixel (*x*, *y*) from $mdLBP_{t2^n}(x,y)$ is defined as,

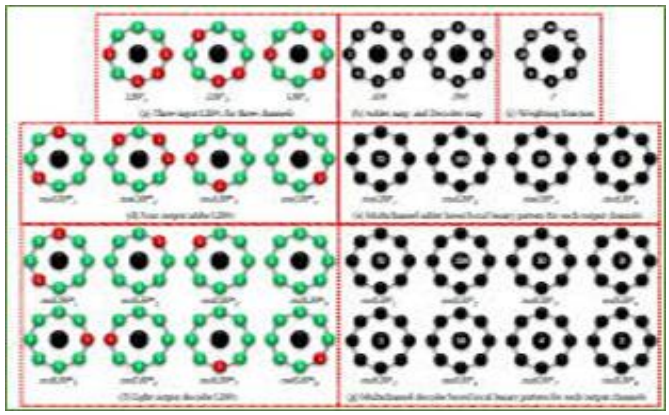

Figure 7. Computation of based LBP and multichannel decoder-based LBP for c=3 and N=8

$$ndLBP_{t2}(x,y) = \sum_{n-1}^{N} mdLBP_{t2}^n(x,y) \times f^n \text{ multi} - \text{channel adder} \quad (6)$$

And then, the feature vectors are computed by applying the histogram function to the resulting adder-channel (i.e., maLBPt1) and the decoder-channel (i.e., mdLBPt2), respectively. Computation of LBP was shown in Figure 7.

3.5 Color features extraction

This research presents a CBIR approach based on the extracted color features. One of the most comprehensive elements is color, which affects an image's foreground, background, and objects. Additionally, resistant to rotation and picture translation is color. Additionally, different color properties are used in a variety of applications. The color space recognizes a specific combination of color methods and the mapping function.

The first and last photographs obtained are shown once the color edge has been found. In this case, it is essential to consider the distance between the database photos and the feature vector of the image provided as the query. If there is a sufficiently small distance between the query picture vector feature and the database images, the corresponding image in the database will be selected as a similar image. Instead of using an exact match, searches are frequently conducted on parity. Additionally, the Manhattan distance is indexed using the index of analogy. The search's outcomes are consequently arranged based on the same index.

3.6 Shape features extraction

The main objective of shape feature extraction is to capture the shape details of the various image elements, such as moment, region, boundary, etc. This extraction makes storing, transmitting, comparing and identifying the shape easier. The shape must have properties that can withstand translation, scaling and rotation. Research has been done to find the best way to pinpoint the properties of shape that would make it possible to store, transmit, or recognize the shape. In this sense, no mathematical change is involved in the selected shape attributes. The RGB color image is converted to a grayscale image to extract the shape features. The colored image has three values for every pixel.

The median filter is employed during the preprocessing stage to reduce noise. The speckle, pepper, and salt noise are reduced when the median filter is used. Additionally, the median filter is used when the blurring of edges is undesirable since it helps maintain tiny details and sharp edges in digital photographs. Almost all of the noisy data in the image is reduced when the median filter is used. To separate the pixels with extremely similar values and ignore undecided pixels from the grey image, the neuromorphic clustering algorithm is next applied.

3.7 Texture features extraction

The GLCM algorithm, which may be seen as a matrix with two dimensions of combined similarity among pairs of pixels and a distance d among them in a particular direction, is a trustworthy and effective way of classifying images using statistical analysis. 14 characteristics were retrieved and specified from the GLCM and used to categorize texture features.

1. Creating a grayscale version of the color image.
2. A 5×5 Gaussian filter is applied to the input image.
3. Blocks of the filtered Image measuring 4×4 are divided up.
4. GLCM calculates the energy, SD, mean value, homogeneity, and contrast for every block.
5. These properties are computed in 4 directions: diagonal (45 and 135 degrees), vertical (0 degrees), and horizontal (90 degrees).
6. The database contains the features that were extracted.

4. RESULTS AND DISCUSSION

This part examines the distance measure utilized in this paper, just as the assessment models used to show the improved enactment of the proposed method.

4.1 Estimation of distance

The distance between the lecture vectors of images and feature vectors of the query image in the dataset is contrasted with tracking down by the most comparative images by the query image, as indicated by the idea of CBIR. There are different distance measures accessible for this reason, for example,

- The Euclidean distance
- The Chi-Square distance
- The Canberra distance
- The L1 or Manhattan distance
- The Cosine distance
- The D1 distance

The Euclidean distance

The Euclidean distance is the most accurate way to measure the distance among two points.

Manhattan distance

It determines the absolute distinction between two points and is also known as the Manhattan distance or L1 distance.

Cosine distance

Cosine similarity is generally used as a metric for measuring distance when the magnitude of the vectors does not matter.

Chi-square distance

Chi-square distance calculation is a statistical method that generally measures the similarity between 2 feature matrices.

Canberra distance

The city block distance metric provides a high value for two identical photos, causing similar images to be dissimilar. Therefore, the difference between each feature pair is normalized by dividing it by the sum of the two feature pairs.

The proposed outcomes are given below to show that, for the test, five classifications with 20 images in each are available with the Corel 1k source. The input images form Corel 1k dataset is described in Figure 8. Cbir-50 dataset also utilized in this paper.

Figure 8. Corel 1K dataset with 5 categories having 20 images to each category

The outcome of the Local Binary Pattern for a query image and recovered images are displayed in Figure 9.

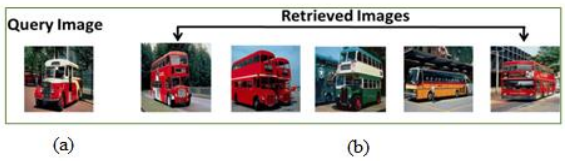

Figure 9. (a) Input image (b) Retrieved images for (LBP)

The outcomes on the multichannel adder-based LBP are shown in Figure 10.

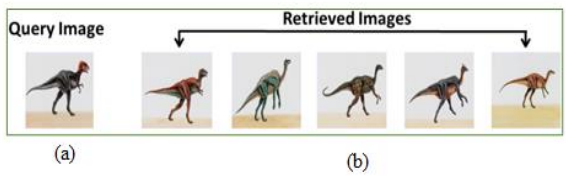

Figure 10. (a) Input image (b) Retrieved images for (maLBP)

The outcomes on the multichannel decoder-based LBP are shown in Figure 11.

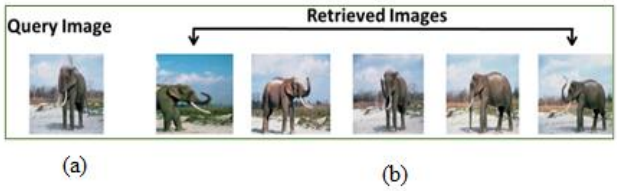

Figure 11. (a) Input image (b) Retrieved images for (mdLBP)

The outcomes of the suggested method, Median-Binary Pattern are shown in Figure 12.

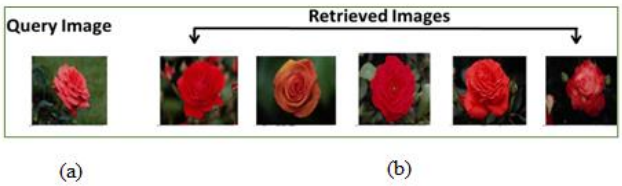

Figure 12. (a) Input images (b) Retrieved images for (MBP)

The outcomes of the suggested method, Median-Binary Pattern are shown in Figure 13.

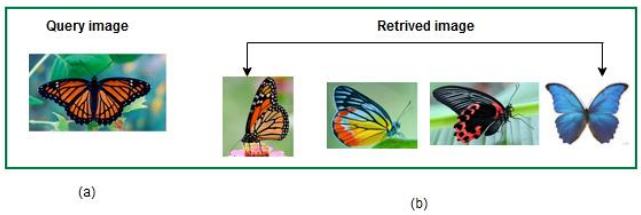

Figure 13. (a) Input images (b) Retrieved images for (MBP)

The outcomes of the suggested method, Median-Binary Pattern are shown in Figure 14.

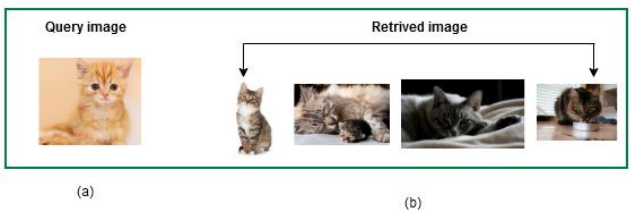

Figure 14. (a) Input images (b) Retrieved images for (MBP)

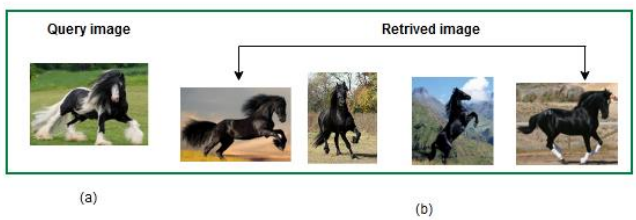

Figure 15. (a) Input images (b) Retrieved images for (MBP)

The outcomes of the suggested method, Median-Binary Pattern are shown in Figure 15.

4.2 Assessment criteria

To compute the average recovery precision (ARP) and average recovery rate (ARR), we should consider each image in the dataset as a query image and track down the most comparable images as query images. The following is how the ARP and ARR are characterized:

$$ARP = \frac{\sum_{i=1}^{C} AP(i)}{C} \quad \& \quad ARP = \frac{\sum_{i=1}^{C} AR(i)}{C} \tag{7}$$

Here C signifies the number of classes in the dataset and AP- average precision and AR- the average recall of a specific classification in the dataset. The AP and AR for the i^{th} class are characterized as follows,

$$AP(i) = \frac{\sum_{i=1}^{Ci} \Pr(j)}{C_i} \quad \& \quad AR(i) = \frac{\sum_{i=1}^{Ci} \mathrm{Re}(j)}{C_i} \tag{8}$$

Here C1 is the total count of images in the dataset's i^{th} classification, Pr and Re indicates recall and precision for a query image and is characterized as below,

$$\Pr(K) = \frac{NS}{NR} \quad \& \quad \mathrm{Re}(K) = \frac{NS}{ND} \tag{9}$$

Here NS means the total of related recovered pictures, NR indicates the total of recovered pictures, and ND signifies the total count of comparative pictures in the dataset.

The ARP and ARR were determined utilizing the dataset's image outcomes. Table 1 shows the AP and AR for the five classifications portrayed in Figure 12.

The ARP and ARR for the Corel 1k dataset with five categories are shown in Figure 16. The x-axis represents the methods of binary patterns such as (LBP, maLBP, mdLBP) and noise-robust binary patterns is (MBP). The method of binary patterns LBP is attained the ARP and the ARR as 49.4, and 23.6, malBP has achieved the ARP and ARR is 79.7 and 38.75, mdLBP is achieved ARP and ARR is 83.1, 40.5. Next, the method of Noise Robust Binary Patterns is MBP has attained the ARP and ARR is 68.1 and 33.55.

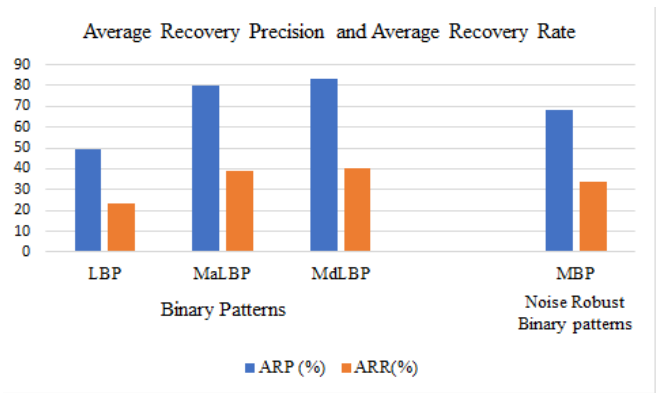

Figure 16. Average recovery precision and average recovery rate

Table 1. The average precision and recalls for five classifications (Beaches, Monuments, Buses, Dinosaurs, and Elephants)

Methods		Average Precision (AP) and Average Recall (AR)									
		Beaches		Monuments		Buses		Dinosaurs		Elephants	
		AP1	AR1	AP2	AR2	AP3	AR3	AP4	AR4	AP5	AR5
Energy Patterns	LBP	28	13.5	42.5	22.75	42.5	21.75	95	46.5	42	20.5
	MaLBP	60.25	28.25	91	44.5	61.5	30.25	96	46	92.5	45.25
	MdLBP	72	35	90.25	43.25	64	31	97	47.5	93	45.5
Noise Robust Binary Pattern	MBP	31	18	93	45.5	79	38.5	82	40	55.5	26.75

5. CONCLUSION

The median binary pattern is recommended in this paper to make the framework noise-robust. The proposed strategy was assessed using image recovery by employing the Corel 1k dataset, in which we thought about five classes, specifically Beaches, Monuments, Buses, Dinosaurs, and Elephants, each with 20 images. Improved performance is perceived when the outcomes are registered as far as ARP and ARR. This paper ponders upon impulsive noise for investigation purposes. The investigational outcomes were differentiated to other models that had been previously developed. Our system is successful and promising because it has an average precision that is higher than that of the currently offered models. Future research should include a deeper analysis of the current approach using various datasets and various approaches. Finding a good way to train the mapping across feature vector spaces so that the error of a preset distance function is reduced would be a further interesting research area.

REFERENCES

[1] Reshma, C., Patil, A.M. (2012). Content based image retrieval using color and shape features. International Journal of Advanced Research in Electrical, Electronics and Instrumentation Engineering, 1(5): 386-392.

[2] Agarwal, M., Singhal, A., Lall, B. (2019). Multi-channel local ternary pattern for content-based image retrieval. Pattern Analysis and Applications, 22: 1585-1596. https://doi.org/10.1007/s10044-019-00787-2

[3] Murala, S., Maheshwari, R.P., Balasubramanian, R. (2012). Directional local extrema patterns: A new descriptor for content based image retrieval. International Journal of Multimedia Information Retrieval, 1(3): 191-203. https://doi.org/10.1007/s13735-012-0008-2

[4] Murala, S., Maheshwari, R.P., Balasubramanian, R. (2012). Local tetra patterns: A new feature descriptor for content-based image retrieval. IEEE Transactions on Image Processing, 21(5): 2874-2886. https://doi.org/10.1109/TIP.2012.2188809

[5] Liu, G.H., Yang, J.Y., Li, Z. (2015). Content-based image retrieval using computational visual attention model. Pattern Recognition, 48(8): 2554-2566. https://doi.org/10.1016/j.patcog.2015.02.005

[6] Datta, R., Li, J., Wang, J.Z. (2005). Content-based image retrieval: Approaches and trends of the new age. In Proceedings of the 7th ACM SIGMM International Workshop on Multimedia Information Retrieval, pp. 253-262. https://doi.org/10.1145/1101826.1101866

[7] Song, Y.J., Park, W.B., Kim, D.W., Ahn, J.H. (2004). Content-based image retrieval using new color histogram. In Proceedings of 2004 International Symposium on Intelligent Signal Processing and Communication Systems, 2004. ISPACS 2004, Seoul, South Korea, pp. 609-611. https://doi.org/10.1109/ISPACS.2004.1439129

[8] Pawar, P., Belagali, P.P. (2015). Image retrieval technique using local binary pattern (LBP). International Journal of Science and Research, 4(7): 1440-1443.

[9] Pass, G., Zabih, R. (1996). Histogram refinement for content-based image retrieval. In Proceedings Third IEEE Workshop on Applications of Computer Vision. WACV'96, Sarasota, FL, USA, pp. 96-102. https://doi.org/10.1109/ACV.1996.572008

[10] Ghahremani, M., Ghadiri, H., & Hamghalam, M. (2021). Local features integration for content-based image retrieval based on color, texture, and shape. Multimedia Tools and Applications, 80(18): 28245-28263.

[11] Kumar, M. S., Rajeshwari, J., Rajasekhar, N. (2022). Exploration on Content-Based Image Retrieval Methods. In Pervasive Computing and Social Networking: Proceedings of ICPCSN 2021 (pp. 51-62). Springer Singapore.

[12] Ojala, T., Pietikäinen, M., Harwood, D. (1996). A comparative study of texture measures with classification based on featured distributions. Pattern Recognition, 29(1): 51-59. https://doi.org/10.1016/0031-3203(95)00067-4

[13] Rassem, T.H., Khoo, B.E. (2014). Completed local ternary pattern for rotation invariant texture classification. The Scientific World Journal, 2014: 373254. https://doi.org/10.1155/2014/373254

[14] Guo, Z., Zhang, L., Zhang, D. (2010). A completed modeling of local binary pattern operator for texture classification. IEEE Transactions on Image Processing, 19(6): 1657-1663. https://doi.org/10.1109/TIP.2010.2044957

[15] Srivastava, V., Purwar, R. (2018). An extension of local mesh peak valley edge based feature descriptor for image retrieval in bio-medical images. ADCAIJ: Advances in Distributed Computing and Artificial Intelligence Journal, 7(1): 77-89.

[16] Li, J., Wang, J.Z. (2003). Automatic linguistic indexing of pictures by a statistical modeling approach. IEEE Transactions on Pattern Analysis and Machine Intelligence, 25(9): 1075-1088. https://doi.org/10.1109/TPAMI.2003.1227984

[17] Kylberg, G., Sintorn, I.M. (2013). Evaluation of noise robustness for local binary pattern descriptors in texture classification. EURASIP Journal on Image and Video Processing, 2013: 1-20. https://doi.org/10.1186/1687-5281-2013-17

[18] Hafiane, A., Seetharaman, G., Zavidovique, B. (2007). Median binary pattern for textures classification. ICIAR, 4633: 387-398.

[19] Tzelepi, M., Tefas, A. (2018). Deep convolutional learning for content based image retrieval. Neurocomputing, 275: 2467-2478. https://doi.org/10.1016/j.neucom.2017.11.022

[20] Saritha, R.R., Paul, V., Kumar, P.G. (2019). Content based image retrieval using deep learning process. Cluster Computing, 22: 4187-4200. https://doi.org/10.1007/s10586-018-1731-0

[21] Monowar, M.M., Hamid, M.A., Ohi, A.Q., Alassafi, M.O., Mridha, M.F. (2022). AutoRet: A self-supervised spatial recurrent network for content-based image retrieval. Sensors, 22(6): 2188. https://doi.org/10.3390/s22062188

[22] Yousuf, M., Mehmood, Z., Habib, H.A., Mahmood, T., Saba, T., Rehman, A., Rashid, M. (2018). A novel technique based on visual words fusion analysis of sparse features for effective content-based image retrieval. Mathematical Problems in Engineering, 2018: 2134395. https://doi.org/10.1155/2018/2134395

[23] Zhou, J.X., Liu, X.D., Xu, T.W., Gan, J.H., Liu, W.Q. (2018). A new fusion approach for content based image retrieval with color histogram and local directional pattern. International Journal of Machine Learning and Cybernetics, 9: 677-689. https://doi.org/10.1007/s13042-016-0597-9